APEM journal
Advances in Production Engineering & Management **ISSN 1854-6250**
Volume 8 | Number 2 | June 2013 | pp 107–115 Journal home: apem-journal.org
http://dx.doi.org/10.14743/apem2013.2.158

Investigation on conformal cooling system design in injection molding

Hsu, F.H.[a,*], **Wang, K.**[a], **Huang, C.T.**[a], **Chang, R.Y.**[b]

[a]CoreTech System (Moldex3D) Co., Ltd., ChuPei City, Hsinchu 302, Taiwan
[b]Department of Chemical Engineering, National Tsing-Hua University, Hsinchu 30043, Taiwan

ABSTRACT

Most advanced technologies developed nowadays focus on issues such as minimizing manufacturing cost and improving product quality. Cooling system design is one of the most critical factors to reduce cycle time. Conformal cooling is the concept which can reduce cooling time and improve product quality as well. However, cooling system layout is restricted by traditional molding method. For cavities with irregular geometry, the distance between cooling channels and cavity may vary throughout the part. This causes local heat accumulation and some product defects such as sink mark and warpage. By using some non-conventional methods such as laser sintering, cooling channels can get closer to the cavity surface than using traditional method. This leads to a shorter cooling time. The current study uses a true three dimensional simulator to predict cooling time and compare the results from a conventional and a conformal cooling design. The results also show flow behavior inside cooling channels which provide important indices for cooling system design revision. With a shorter cycle time and an improved product quality, conformal cooling has a great potential in injection molding industry.

ARTICLE INFO

Keywords:
Injection molding
Conformal cooling
Cooling design
Simulation

**Corresponding author:*
andrewhsu@moldex3d.com
(Hsu, F.H.)

1. Introduction

A general trend in injection molding industry is to reduce manufacturing cost and improve product quality. Injection molding cycle time has a direct relation with manufacturing cost. During the whole injection molding cycle, cooling stage usually takes the longest time. Thus, reducing cooling time also means cost saving. Common factors related to cooling time are cooling system design, mold material, coolant type, coolant temperature, and flow rate etc. Among these factors, cooling system design variation is possibly the most difficult part by using traditional molding method.

However, by using techniques such as three dimensional printing and laser sintering processes, conformal cooling channel is able to be manufactured and getting popular. Dalgarno and Stewart used indirect selective laser sintering method for conformal cooling channel manufacturing. In the two cases they tested, cooling time was drop up to 50 % [1]. Three dimensional printing is another technique developed by Sachs et al. in MIT [2]. In their experiment, the results with conformal cooling design show better control on mold temperature than those without it.

As to the design algorithm of conformal cooling channels, there is a general design rule among distance from cavity to cooling channel, distance between cooling channels and cooling channel diameter [3]. For cooling channel layout, numerous studies have provided different al-

gorithms on building an optimized cooling channel [4-7]. In this research, we use two models with numerical simulations to demonstrate the effects of conformal cooling designs on tool temperature and product deformation.

2. Simulation detail

In this study, the fluids are considered to be incompressible, Newtonian (for water) or generalized Newtonian (for polymer melt). The governing equations for 3D transient non-isothermal motion are:

$$\frac{\partial \rho}{\partial t} + \nabla \cdot \rho \boldsymbol{u} = 0 \tag{1}$$

$$\frac{\partial}{\partial t}(\rho \boldsymbol{u}) + \nabla \cdot (\rho \boldsymbol{u}\boldsymbol{u} + \tau) = -\nabla p + \rho g \tag{2}$$

$$\rho C_p \left(\frac{\partial T}{\partial t} + \boldsymbol{u} \cdot \nabla T\right) = \nabla (k \nabla T) + \eta \dot{\gamma}^2 \tag{3}$$

where $\boldsymbol{u}$ is velocity vector, T is temperature, t is time, p is pressure, τ is stress tensor, ρ is density, η is viscosity, k is thermal conductivity, C_p is specific heat and $\dot{\gamma}$ is shear rate. For the polymer melt, the stress tensor can be expressed as:

$$\tau = -\eta(\nabla \boldsymbol{u} + \nabla \boldsymbol{u}^T) \tag{4}$$

The modified-Cross model with Arrhenius temperature dependence is employed to describe the viscosity of polymer melt:

$$\eta(T, \dot{\gamma}) = \frac{\eta_0(T)}{1 + (\eta_0 \dot{\gamma}/\tau^*)^{1-n}} \tag{5}$$

with

$$\eta_0(T) = BExp\left(\frac{T_b}{T}\right) \tag{6}$$

where n is the power law index, η_0 is the zero shear viscosity, τ^* is the parameter that describes the transition region between zero shear rate and the power law region of the viscosity curve.

For the flow inside cooling channels, an incompressible Raynolds-averaged Navier-Stoke (RANS) model was applied [8]:

$$\frac{\partial \overline{u}_\iota}{\partial x_i} = 0$$
$$\rho \frac{\partial \overline{u}_\iota}{\partial t} + \rho \frac{\partial \overline{u}_\iota \overline{u}_j}{\partial x_j} = g_i - \frac{\partial \bar{p}}{\partial x_i} + \frac{\partial \tau_{ij}}{\partial x_j} + \frac{\partial \tau_{ij}^t}{\partial x_j} \tag{7}$$

where

$$\tau_{ij} = \mu \left(\frac{\partial \overline{u}_\iota}{\partial x_j} + \frac{\partial \overline{u}_j}{\partial x_i}\right)$$
$$\tau_{ij}^t = -\rho \overline{u_\iota' u_j'} \tag{8}$$

Term $\overline{u_i'u_j'}$ is called turbulent stress. To calculate this term, the Boussinesq hypothesis (linear eddy viscosity model) was applied to make this term analogous to molecular shear. Introducing $k-\varepsilon$ two equation model, we have:

$$-\rho\overline{u_i'u_j'} = \mu_t\left(\frac{\partial\overline{u_i}}{\partial x_j}+\frac{\partial\overline{u_j}}{\partial x_i}\right)-\frac{2}{3}\left(K+\mu_t\frac{\partial\overline{u_k}}{\partial x_k}\right)\delta_{ij} \tag{9}$$

$$K=\frac{1}{2}\left(\overline{u_1'^2}+\overline{u_2'^2}+\overline{u_3'^2}\right) \qquad \mu_t=\rho C_\mu\frac{K^2}{\varepsilon} \tag{10}$$

where K is the turbulence kinetic energy and μ_t is the eddy viscosity, ε is dissipation. Cooperate eq. 11 and eq. 12 into eq. 8, we have the new momentum equation:

$$\rho\frac{\partial\overline{u_i}}{\partial t}+\rho\frac{\partial\overline{u_i}\overline{u_j}}{\partial x_j}=g_i-\frac{\partial}{\partial x_i}\left(\bar{p}+\frac{2}{3}K\right)+\frac{\partial}{\partial x_j}\left((v+v_i)\left(\frac{\partial\overline{u_j}}{\partial x_i}+\frac{\partial\overline{u_i}}{\partial x_j}\right)\right) \qquad v_t=C_\mu\frac{k^2}{\bar{\varepsilon}} \tag{11}$$

The transport equations of K and ε are:

$$\begin{aligned}\frac{\partial \mathrm{K}}{\partial t}+\overline{u_j}\frac{\partial \mathrm{K}}{\partial x_j}&=\frac{\partial}{\partial x_j}\left(\frac{v_t}{\sigma_K}\frac{\partial \mathrm{K}}{\partial x_j}+v\frac{\partial \mathrm{K}}{\partial x_j}\right)+v_tG-\bar{\varepsilon}\\ \frac{\partial\bar{\varepsilon}}{\partial t}+\overline{u_j}\frac{\partial\bar{\varepsilon}}{\partial x_j}&=\frac{\partial}{\partial x_j}\left(\frac{v_t}{\sigma_z}\frac{\partial\bar{\varepsilon}}{\partial x_j}+v\frac{\partial\bar{\varepsilon}}{\partial x_j}\right)+C_{z1}\frac{\bar{\varepsilon}}{K}v_tG-C_{z2}\frac{\bar{\varepsilon}^2}{K}\end{aligned} \tag{12}$$

where

$$\begin{aligned}G&=\left(\frac{\partial\overline{u_i}}{\partial x_j}+\frac{\partial\overline{u_j}}{\partial x_i}\right)\frac{\partial\overline{u_i}}{\partial x_j}\\&=2\left(\left[\frac{\partial u}{\partial x}\right]^2+\left[\frac{\partial v}{\partial y}\right]^2+\left[\frac{\partial w}{\partial z}\right]^2\right)+\left(\frac{\partial u}{\partial y}+\frac{\partial v}{\partial x}\right)^2+\left(\frac{\partial u}{\partial z}+\frac{\partial w}{\partial x}\right)^2+\left(\frac{\partial w}{\partial y}+\frac{\partial v}{\partial z}\right)^2\end{aligned} \tag{13}$$

The empirical constants are:

$$\left(\sigma_K, C_\mu, \sigma_\varepsilon, C_{\varepsilon1}, C_{\varepsilon2}\right)=(1.00, 0.09, 1.30, 1.44, 1.92)$$

The numerical tool, Moldex3D, uses a hybrid finite-difference/control volume/finite element method. Time step selection has an important effect on accuracy and calculating speed. An internal parameter was carefully chosen to have a good balance on accuracy and efficiency.

3. Case study

Two models were tested in this study. The models were both built with three dimensional solid mesh. The total element numbers are 1.05M and 9.33M respectively. Model 1 is validated with experimental data. Model 2 is used to show the three-dimensional calculation inside cooling channels.

Model 1 geometry: This is a machine tool cover model. Two cooling systems were designed and compared to each other (Fig. 1).

Model 1 material: The material used is ABS (Techno ABS350). Ejection temperature is 97 °C. The modified Cross model is used for modeling the viscosity of polymer melt as functions of pressure, temperature, and shear rate.

Model 1 processing conditions: The filling time is specified as 0.7 s. Maximum injection pressure is specified as 252 MPa. Melt temperature at sprue entrance is 225 °C. Mold temperature is

60 °C. Packing time is 5 s. Packing pressure is 252 MPa. Cooling time is 20 s. Mold open time is 5 s. Air temperature is 25 °C. Cycle time is 30.7 s.

Model 2 geometry: There is a syringe-shape model as shown in Fig. 2. The dimension is 105.22 mm (W) × 162.23 mm (L) × 44.51 mm (H). The average product thickness is 3 mm. Fig. 3 shows the conformal cooling channel layouts. Fig. 3 also shows the dimension of conformal cooling channel. The twin-spiral channel has a diameter of 3mm. The distance between the centerlines of the channels (a) is 12 mm which is four times of the channel diameter. The distances between center of channels and cavity (c1 and c2) are 3 mm and 10 mm respectively. These parameters are within the scope of general design rules [3].

Model 2 material: The material used is PC (Teijin Panlite L-1225). Ejection temperature is 135 °C.

Model 2 processing conditions: The filling time is specified as 0.3 s. Maximum injection pressure is specified as 212 MPa. Melt temperature at sprue entrance is 290 °C. Mold temperature is 100 °C. Packing time is 2.5 s. Packing pressure is 212 MPa. Cooling time is 20 s. Mold open time is 5 s. Air temperature is 25 °C. Cycle time is 27.8 s.

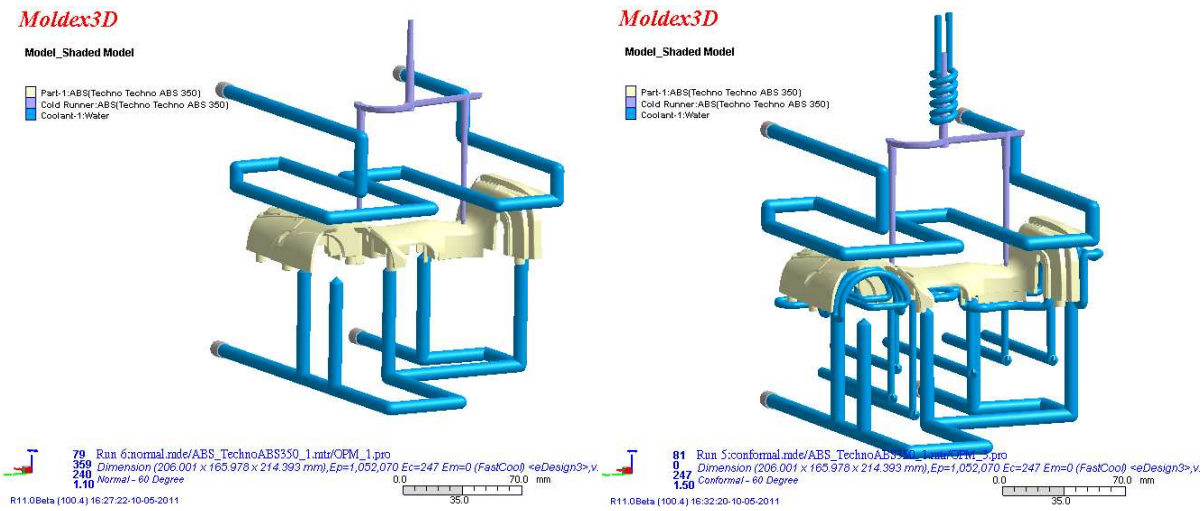

Fig. 1 The machine tool cover model: w/ normal cooling (left), w/ conformal cooling (right)

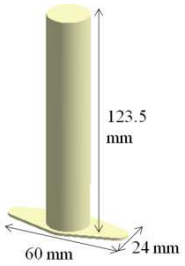

Fig. 2 The syringe model

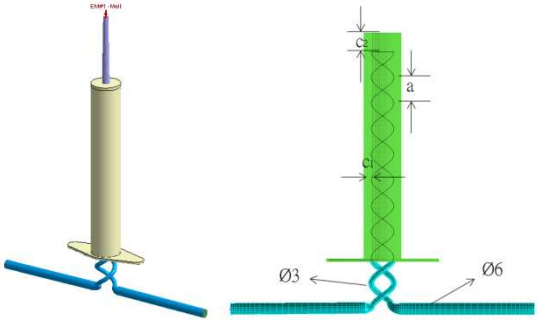

Fig. 3 Conformal cooling design

4. Results and discussion

Let us first discuss the results from model 1. Fig. 4 shows the part surface temperature distribution at the end of cooling (EOC). The two pictures were set at the same temperature range. This is the view from the core side where major difference occurs due to the cooling system designs. We can observe that conformal cooling can lower the part surface temperature significantly.

Fig. 5 shows the cooling efficiencies of channels in normal and conformal designs. The conformal cooling channel at core side absorbs 53.7 %

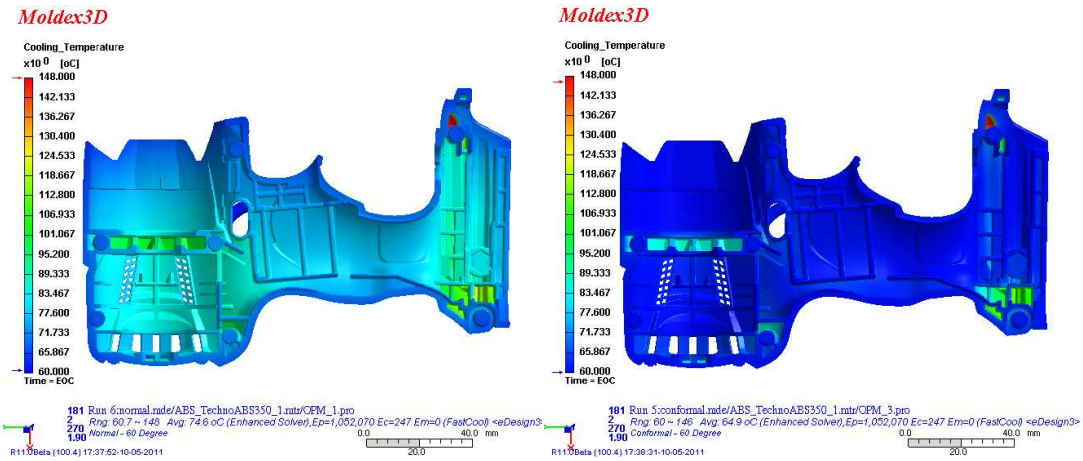

Fig. 4 EOC part surface temperature distribution: normal cooling (left), conformal cooling (right)

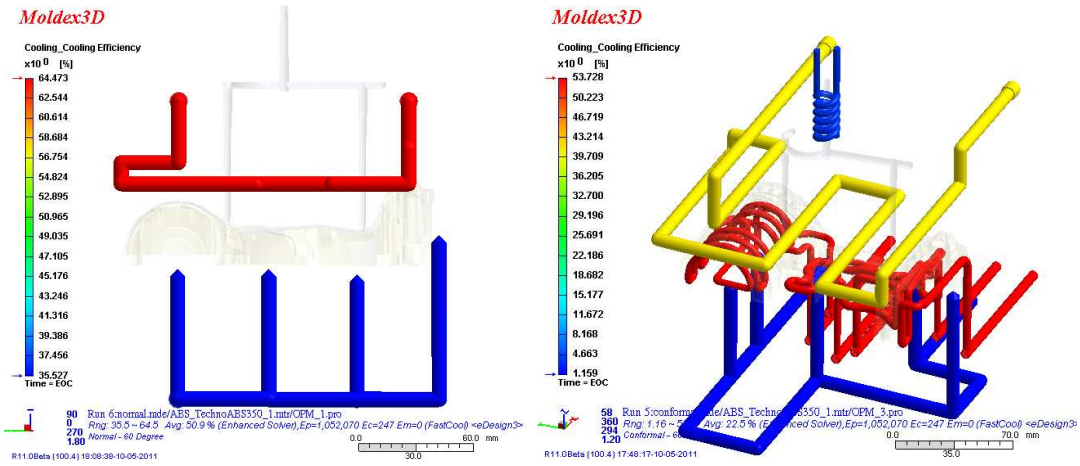

Fig. 5 Cooling efficiency: normal (left), conformal (right)

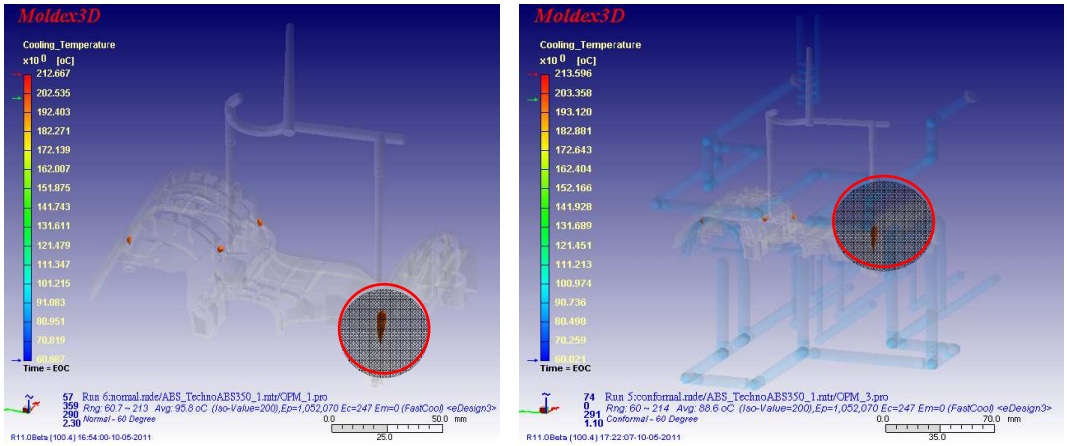

Fig. 6 Part interior temperature at EOC: normal (left), conformal (right)

of the total heat. Fig. 6 shows the interior temperature at the end of cooling. The brown areas are the places where temperature is over 200 °C. It is obvious that the temperature is not much different since the heat spots (shown in circles) do not have any cooling channel pass by for each cooling system design. The results are also correspondent with the cooling time results. The maximum cooling time for normal cooling design is 110.3 s and 105.6 s for the conformal design. However, in reality, it does not need such a long time to eject the part. This simulation had been validated with experiments. Fig. 7 shows photos of the actual part. The red circle in the right figure indicates the location of sink mark. The ejection criteria is no sink mark at this area where the heat spot located. From the actual molding results, 30 s cooling is needed for the normal design while only 20 s is needed to avoid sink mark appearance. Fig. 8 shows the comparison – cooling time distribution is almost identical for the two cases.

Fig. 7 Product photo (left), sink mark area (right)

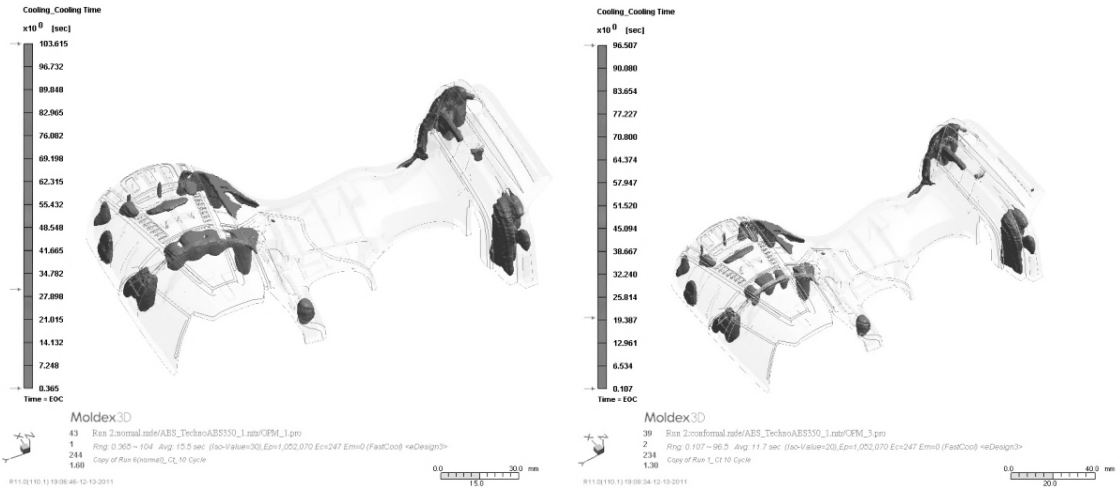

Fig. 8 Cooling time results: normal w/ 30 s cooling (left), conformal w/ 20 s cooling (right)

The second half of the study is to simulate the coolant behavior inside the channels. Model 2 with spiral cooling channel was simulated. Table 1 shows the results comparing the case of no cooling channel and conformal cooling channel. Water temperature is 100 °C and flow rate is 120 cm^3/s. With conformal cooling channel, part temperature, mold temperature difference, cooling time, and thermal displacement are all decreased slightly.

Table 1 Results summary (water temperature = 100 °C)

	No Cooling	w/conformal
EOC part temperature (°C)	101.0–141.7	100.0–135.4
EOC mold temperature (°C)	97.7–125.1	97.7–102.0
Mold temperature difference (°C)	0–38.2	0–32.0
Cooling time (s)	0.3–24.7	0.3–23.5
Total displacement (mm)	0.018–0.202	0.018–0.202

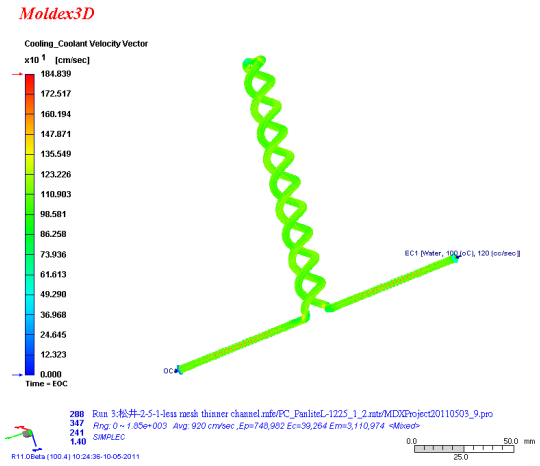

Fig. 9 Coolant velocity vector distribution – conformal cooling channels

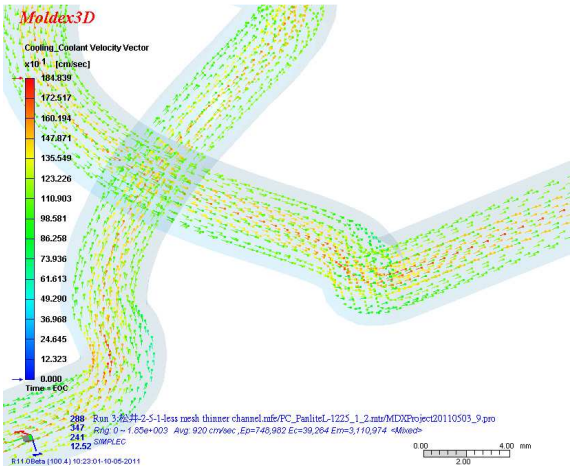

Fig. 10 Coolant velocity vector (enlarged view) – conformal cooling channels

Fig. 9 and Fig. 10 show the three dimensional coolant velocity vector results. In Fig. 9, we can see that the velocity range is from 0 cm^3/s to 1848.4 cm^3/s. The lowest velocity occurs at the cooling channel surfaces. Fig. 10 shows an enlarged view of the velocity vector in the red window shown in Fig. 9. It shows no dead water areas in this cooling system design. By checking velocity results, we can avoid low efficiency cooling system designs in advance.

To further investigate the process parameter effects on cooling efficiency, we change the water temperature and flow rate. We first change the water temperature from 100 °C to 80 °C. From the results shown in Table 2, part temperature, mold temperature difference, cooling time, and thermal displacement are all decreased more significantly than water temperature of 100 °C. For example, cooling time has a 12.8 % improvement. Thus, we can conclude that a lower coolant temperature is helpful in removing heat and improving warpage problem.

We then investigate the flow rate effects on coolant temperature. Fig. 11 and 12 show the coolant temperature at flow rate of 120 cm^3/s. Fig. 13 and 14 show the coolant temperature at flow rate of 12 cm^3/s (ten times slower).

Table 2 Results summary (water temperature = 80 °C)

	No Cooling	w/ conformal
EOC part temperature (°C)	81.6–136.5	80.2–118.9
Mold temperature difference (°C)	0–44.4	0–1.7
Cooling time (s)	0.2–20.3	0.2–17.7
Total displacement (mm)	0.018–0.196	0.016–0.187
Total thermal displacement (mm)	0.059–0.418	0.043–0.341

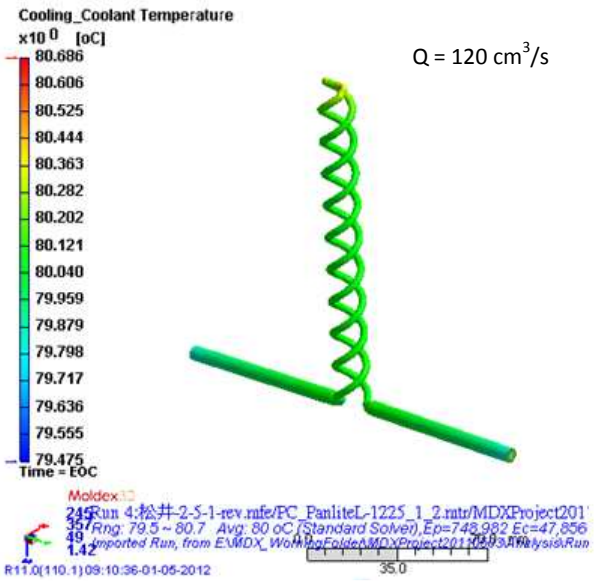

Fig. 11 Coolant temperature (Q = 120 cm³/s)

If we compare Fig. 12 and Fig. 14 (both set at the same temperature range), we can observe that temperature rise effect at water outlet is more significant for a lower flow rate.

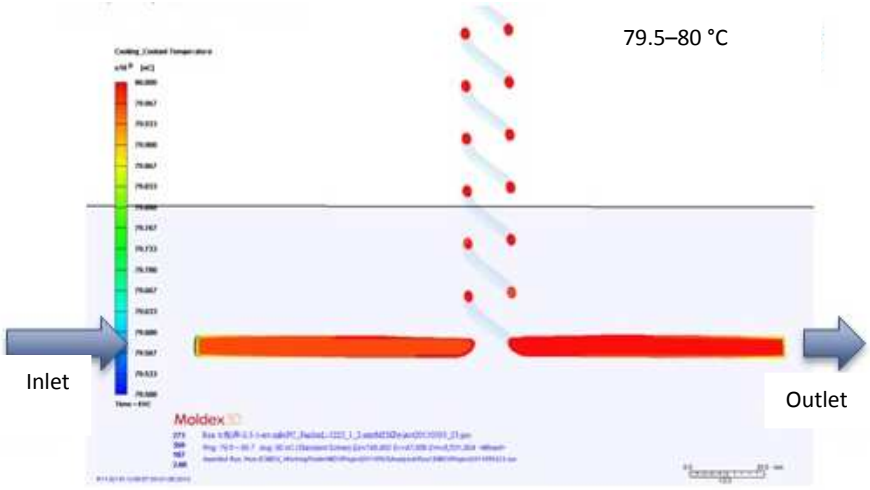

Fig. 12 Coolant temperature (Q = 120 cm³/s, slicing view)

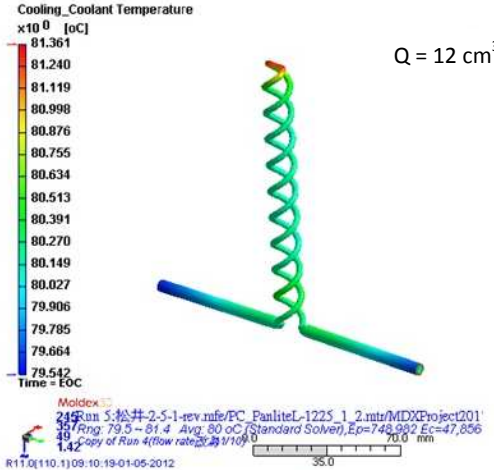

Fig. 13 Coolant temperature (Q = 12 cm³/s)

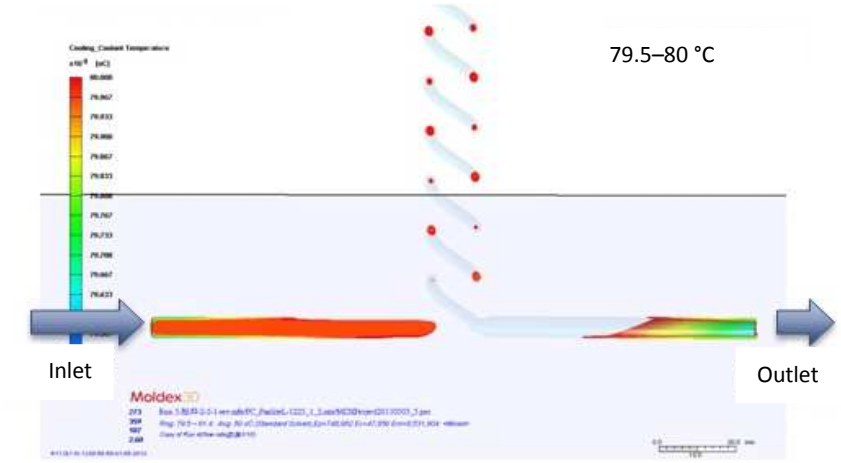

Fig. 14 Coolant temperature (Q = 12 cm^3/s, slicing view)

5. Conclusion

In this paper, we used a three dimensional numerical scheme to present the advantages of conformal cooling design. Two different models were used with a normal and a conformal cooling design individually. The first model was validated with experimental data with good agreement. In the second model, coolant properties were predicted, and property effects were studied (water temperature and coolant flow rate). The results show that conformal cooling is effective in reducing cooling time and product displacement. Some functions from CFD are now embedded in a molding simulator in three dimensional. The prediction of coolant flow behavior is very helpful in understanding cooling channel efficiency as well as cooling system design revision.

Acknowledgement

Special thank for OPM Lab, Japan who provided real case (model 1) molding data in validating the simulation results.

References

[1] Dalgarno, K.W., Stewart, T.D. (2001). Manufacture of production injection mould tooling incorporating conformal cooling channels via indirect selective laser sintering, *Proceeding of the institution of mechanical engineers*, Vol. 215, part B, 1323-1332.
[2] Sachs, E., Wylonis, E., Allen, S., Cima, M., Guo, H. (2000). Production of injection molding tooling with conformal cooling channels using the three dimensional printing process, *Polymer Engineering and Science*, Vol. 40, No. 5, 1232-1247.
[3] Mayer, S. Optimized mould temperature control procedure using DMLS, EOS whitepaper, EOS, from *http://www.compositesworld.com/*, accesed June 20, 2012.
[4] Li, C.L. (2001). A feature-based approach to injection mould cooling system design, *Computer-Aided Design*, Vol. 33, No. 14, 1073-1090, doi: 10.1016/S0010-4485(00)00144-5.
[5] Au, K.M., Yu, K.M. (2007). A scaffolding architecture for conformal cooling design in rapid plastic injection moulding", *The International Journal of Advanced Manufacturing Technology*, Vol. 34, No. 5-6, 496-515.
[6] Park, H.S., Pham, N.H. (2009). Design of conformal cooling channels for an automotive part, *International Journal of Automotive Technology*, Vol. 10, No. 1, 87-93.
[7] Au, K.M, Yu, K.M., Chiu, W.K. (2011). Visibility-based conformal cooling channel generation for rapid tooling, *Computer-Aided Design*, Vol. 43, No. 4, 356-373.
[8] White, F.M. (1991). *Viscous fluid flow*, 2nd ed., McGraw Hill, New York.